

# Meteoroid orbital element distributions at 1 AU deduced from the Harvard Radio Meteor Project observations

A. D. Taylor<sup>1,2</sup> and W. G. Elford<sup>2</sup>

<sup>1</sup>*Durham School, Durham, DH1 4SZ, United Kingdom*

<sup>2</sup>*Department of Physics and Mathematical Physics, University of Adelaide, Adelaide, 5005, South Australia*

(Received October 21, 1997; Revised March 13, 1998; Accepted March 26, 1998)

The orbital element distributions of meteoroids detected during the Harvard Radio Meteor Project, 1968–69 Synoptic Year Program, have been reanalysed to remove selection effects associated with the radar observations. Corrections are made for the observing schedule, antenna beam patterns, the radio diffusion ceiling, speed dependence of ionization production, the flux enhancement due to the Earth's gravity and the probability of encounter with the Earth. These render the eccentricity, aphelion distance, and inclination distributions for meteoroids larger than  $10^{-4}$  g (radius  $\sim 200$   $\mu\text{m}$ ), with orbits that cross the ecliptic near 1 AU.

## 1. Introduction

The 1968–69 Harvard Radio Meteor Project (HRMP) synoptic year observations produced about 20,000 meteor orbits from meteoroids larger than  $10^{-4}$  g (radius  $\sim 200$   $\mu\text{m}$ ). This is a statistically reliable data set from which to determine the distribution of the orbital elements of the meteoroids. An analysis carried out by Sekanina and Southworth (1975) provided such a set of distributions corrected for the biases that the authors considered were associated with the observations and with the probability of encounter with the Earth. It is now known that Sekanina and Southworth used an incorrect velocity bias (Taylor, 1995), made a significant underestimate of the effect of diffusion of meteor trails on their radar detectability (Taylor and McBride, 1997), and took no account of the effect of Faraday rotation on the radar echoes. As a result the distributions of meteoroid orbital elements deduced by Sekanina and Southworth are grossly in error. Revised distributions using the raw data available from the IAU Meteor Data Centre (Lindblad, 1987, 1991) are presented in what follows.

## 2. Meteor Radar Response Function

The majority of radar echoes from meteor trails occur when the trail is orthogonal to the line of sight to the radar station; the echo comes from a region of the trail of the order of one Fresnel zone length about the orthogonal point (for the Harvard Radar this length was 1.1 to 1.5 km). The probability of a meteor trail being detected by radar depends on the electron line density of the ionization in the trail, the orthogonality condition, and the parameters of the radar system. This probability can be determined theoretically by assuming that a unit source of meteors is placed at an array of positions on the celestial sphere. The resultant contour plot of the probability as a function of the celestial coordinates

(radiants) of the meteor sources is known as the 'response function of the radar'. This was determined for the Harvard Radio Meteor system by Elford (1964) and slightly modified by Southworth and Sekanina (1973) to take into account an updated antenna calibration.

## 3. The Data Set

In order to interpret the raw data it is necessary to know (a) the fraction of time that the system was operating, and (b) the relative observing time for each radiant, which when averaged over one day is a function of the declination. The latter function was calculated by Elford and Hawkins (1964). As the log-books for the system operation have not survived (Z. Sekanina, private communication) there is no precise information on the times of operation and thus only a crude correction could be applied for 'down times'. Southworth and Sekanina (1973) report that the synoptic year data set 'comprises nearly uniform coverage of all hours'.

For their study of the orbital element distributions Sekanina and Southworth (1975) restricted the analysis to meteors occurring within the 10% sensitivity contour of the radar beam. Without the detailed operating log showing which of eight receivers were operating at any given time and the details indicating at which stations a given meteor was detected, it has not been possible to confidently recover this 10% contour. We have been forced to omit this correction.

## 4. Initial Radius and Diffusion of the Meteor Trail

The initial radius of a meteor trail and the rapid diffusion of the trail in the atmosphere reduces the amplitude and the duration of a radar meteor echo, and hence its detectability. Both effects are a function of height. As faster meteors ionize at greater heights this selection effect is a function of the speed of the meteor. The detectability of the meteor is also dependent on the pulse repetition rate of the radar, and this bias is also ultimately a function of the meteor speed. The effect of these biases is equivalent to an increase in the minimum electron line density detectable by the radar.

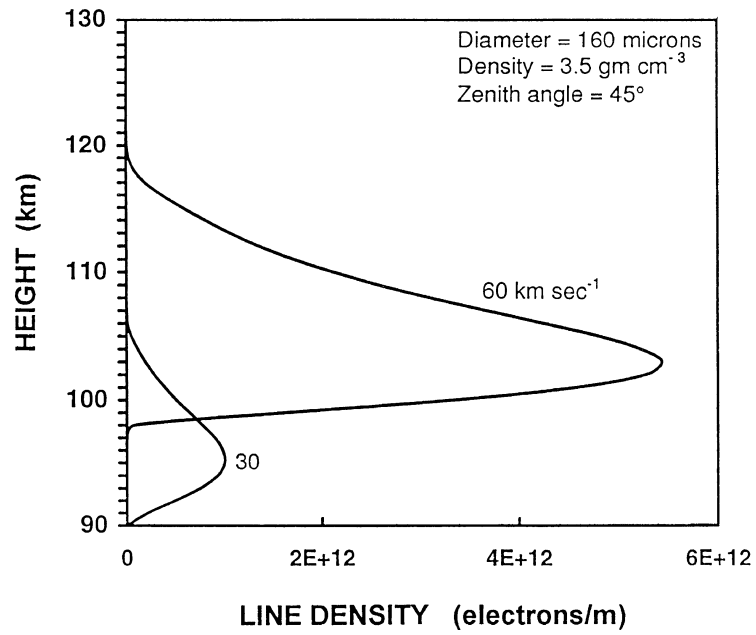


Fig. 1. Effect of the entry speed on the ionisation profile of a stony meteoroid.

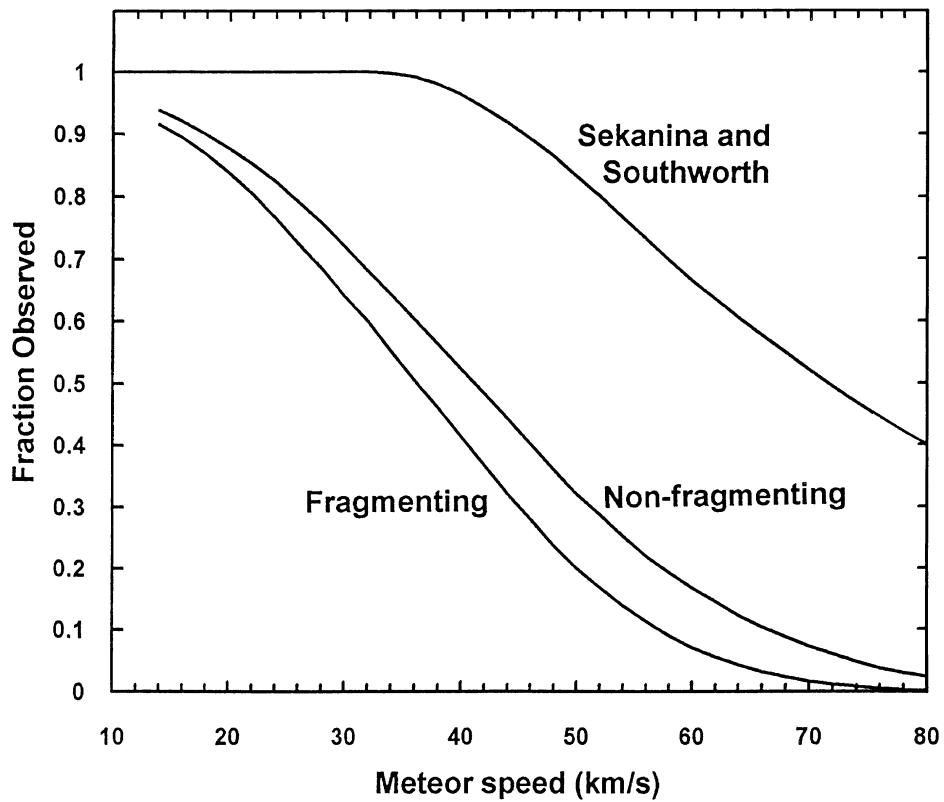


Fig. 2. The probability of detecting a meteor with the Harvard Radio Meteor Project system as a function of the entry speed of the meteoroid. The effect of fragmentation of the incident particle into a limited number of fragments is also shown. Sekanina and Southworth (1975) greatly underestimated the effect of diffusion on radar meteor detectability.

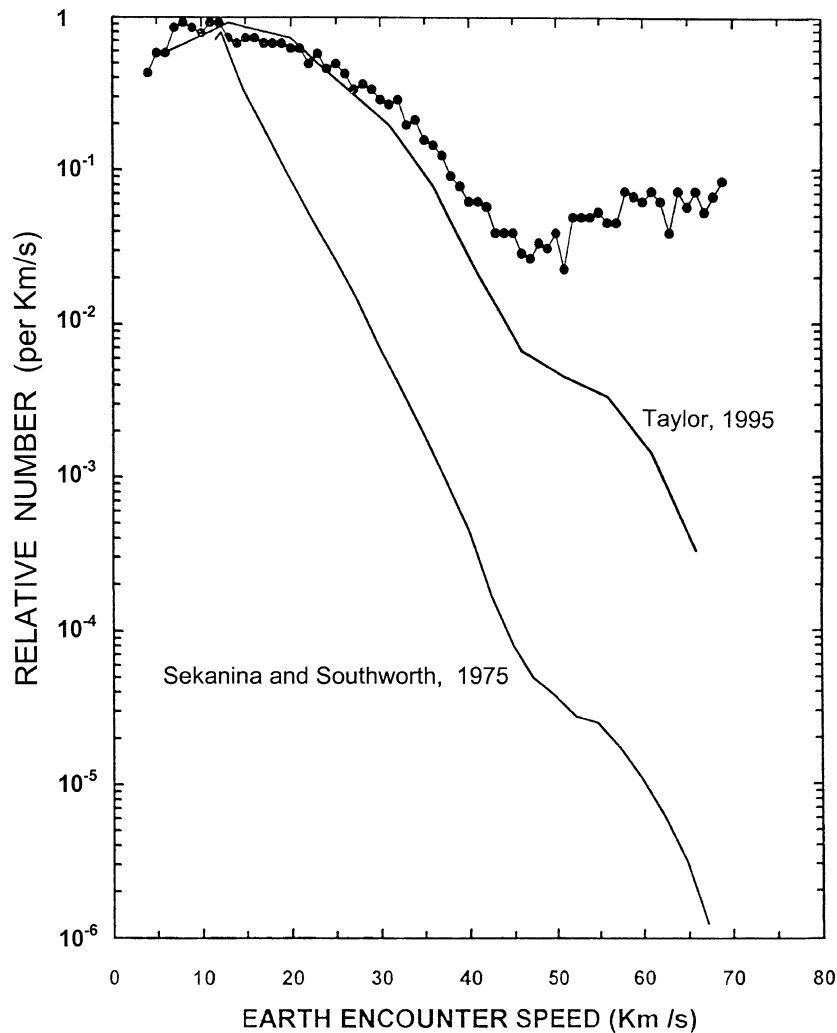


Fig. 3. The speed distribution of meteoroids with masses  $>10^{-4}$  g encountering the Earth, derived from meteors observed during the Harvard Radio Meteor Project 1968–69. The two continuous lines are the original distribution of Sekanina and Southworth (1975) and Taylor's correction (1995) for the effect of velocity on ionisation production during ablation. The filled circles include the effect of diffusion on the radar detectability of a meteor trail, and are based on the raw data, thus allowing a resolution in speed of 1 km/s.

Using a meteor ablation modelling procedure similar to that of Love and Brownlee (1991), but with 1 km increments in height rather than equal increments of time, we generated a series of typical meteor ionization profiles as a function of speed, as is shown in Fig. 1 for two meteoroids that differ only in their entry speed. Convolution of the height dependent detectability of a meteor with the theoretical ionization height profiles gives an estimate of the relative fraction of meteors missed when using the HRMP system. The probability of the detection of meteors with the HRMP as a function of speed due to these atmospheric and sampling effects is shown in Fig. 2 together with the probability-speed dependence calculated by Sekanina and Southworth. Clearly, the earlier analysis grossly underestimated the magnitude of the atmospheric effects on the radar echoes.

Sekanina and Southworth (1975) addressed the possibility of fragmentation of the ablating meteoroids, and based on the HRMP data concluded that the vertical extent of the observed meteor trails was only approximately 60% of that expected for a non-fragmenting meteoroid. To provide an

estimate of the relative influence of meteoroid fragmentation on the observability of meteors with HRMP system, we compressed the vertical extent of the modelled single-body ablation profiles to 60%, leaving the onset of ablation at the same height. The effect of this fragmentation estimate on the detectability of meteors as a function of speed is included in Fig. 2. The compressed ablation profiles are consistent with the theoretical profiles obtained by Taylor *et al.* (1997) when meteoroids are assumed to fragment during ablation, and the resultant ionisation profile is the sum of the profiles of the individual fragments.

From the fragmenting graph in Fig. 2, a weight for the effects discussed in this section can be estimated as a function of the speed of the meteoroid, and applied to each orbit in the data set.

## 5. Electron Line Density, Velocity and Mass

The amount of ionisation produced by an ablating meteoroid is strongly dependent on the speed of the meteoroid. A survey by Bronshten (1983) of laboratory studies of the

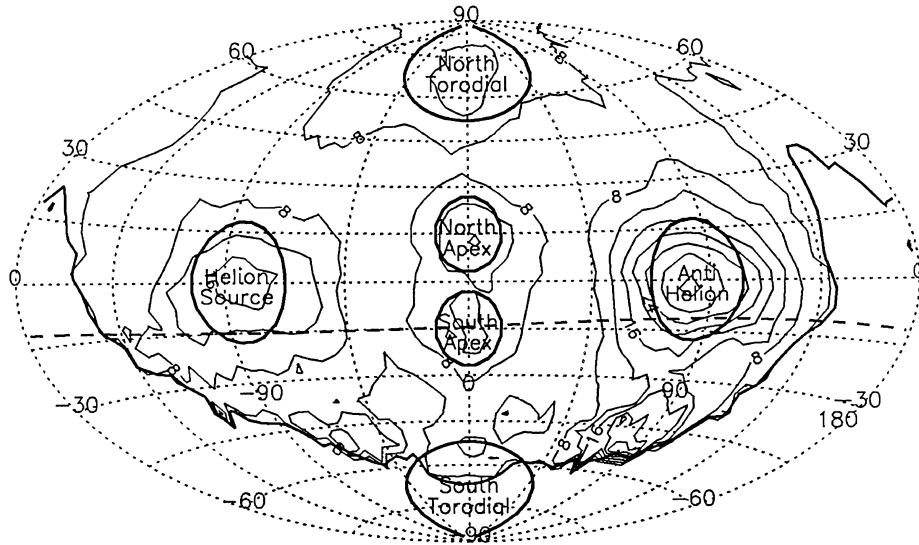


Fig. 4. The radiant distribution of meteoroids with masses  $>10^{-4}$  g encountering the Earth. The coordinate frame places the Earth's Apex at the centre, the solar (Helion) direction at a longitude of  $-90$  degrees, and the north ecliptic pole at  $+90$  degrees. The distribution is based on radar observations (see text) and has been corrected for selection effects associated with the radar detectability of meteors and the atmosphere. The heavy line is the limit of observation of the radar, and radiants south of the dashed line were observed for less than 10% of the time spent observing the region of the celestial north pole. The six radiant sources are overlaid with the one sigma radii appropriate to each source. The contour values are proportional to the number of meteoroids per square degree.

ionization coefficients of atoms that typify chondritic meteoroids indicates that if the mass and speed of a meteoroid are  $m$  and  $V$ , the maximum electron line density has a mass and speed dependence of the form  $mV^b$ , where  $b = 3.75$ . The speed of a meteoroid also has a very significant effect on the height of ablation in the atmosphere as is shown in Fig. 1 for the same stony particle entering the atmosphere at speeds of 30 km/s and 60 km/s.

The radar systems will detect meteors with electron line densities above some minimum limit  $q_{\min}$ . However, in discussing the orbits of meteoroids the statistics are to be related to meteoroids with masses above a certain mass limit  $m$ . For a given velocity,  $V$ , the mass limit  $m_V$  is related to the electron line density limit  $q_{\min}$  by  $q_{\min} \propto m_V V^b$ .

For any velocity interval  $V$  to  $V + \Delta V$  the number of meteoroids,  $N_V$ , greater than a given mass  $m_V$ , is usually expressed by the relation

$$N_V(m > m_V) \propto m_V^{-\alpha} \propto (q_{\min})^{-\alpha} V^{\alpha b}$$

where  $\alpha$  is the cumulative mass index. Sekanina and Southworth (1975) used a value of  $\alpha = 1.36$  which was known for particle masses of order 1 g, and is now considered too large. Grün *et al.* (1985) summarised the meteoroid mass distribution based on a wide range of measurements, including extensive use of spacecraft instruments. We have used their distribution to normalise the number of meteoroids observed in a velocity interval  $V$  to  $V + \Delta V$  to the number observed in a similar interval based on the normalising threshold velocity,  $V_0 = 30$  km/s, chosen to correspond to a mass detection threshold of  $10^{-4}$  g as is appropriate for the HRMP system. In the Grün *et al.* distribution  $\alpha$  varies from 1.0 to 1.2 across the HRMP mass range.

## 6. The Distribution of Meteoroid Speeds

The first analysis of the HRMP data set carried out by Sekanina and Southworth (1975) included a distribution of the speeds of the 14,220 meteoroids corrected for the estimates of the effects of the radar detectability of the meteor trails and the velocity bias on the meteoric ionisation, as deduced by the authors. This distribution has been used extensively by subsequent workers. As stated above we now know that Sekanina and Southworth grossly underestimated the effects of the initial radius and the diffusion of the trails. Further, Taylor (1995) has shown that a typographical error in the computer code used by Sekanina and Southworth caused the flux of high speed meteoroids to be underestimated by a factor of about 100. The Sekanina and Southworth meteoroid velocity distribution and Taylor's initial revision of their distribution is shown in Fig. 3 as full lines. Taylor's revision did not reconsider the height, and hence speed, dependent selection biases addressed in the current work. The effect of including the new correction factors for initial radius of the meteor trail, the diffusion of the ionisation, and fragmentation are shown in Fig. 3 as filled circles. This new analysis was based on the raw data set of 19,698 meteors, and the resolution in velocity was set at 1 km/s.

## 7. Distribution of Meteor Radiants and Orbits

The distribution of the radiants of meteors detected by the Harvard Radio Meteor Project is shown in Fig. 4, where a weight has been applied to each observed radiant for the various selection effects described above. A small correction for the flux enhancement due to the Earth's gravity has also been incorporated. Incomplete coverage of the southern-ecliptic hemisphere necessitates the assumption that the radiant distribution is symmetric about the ecliptic plane.

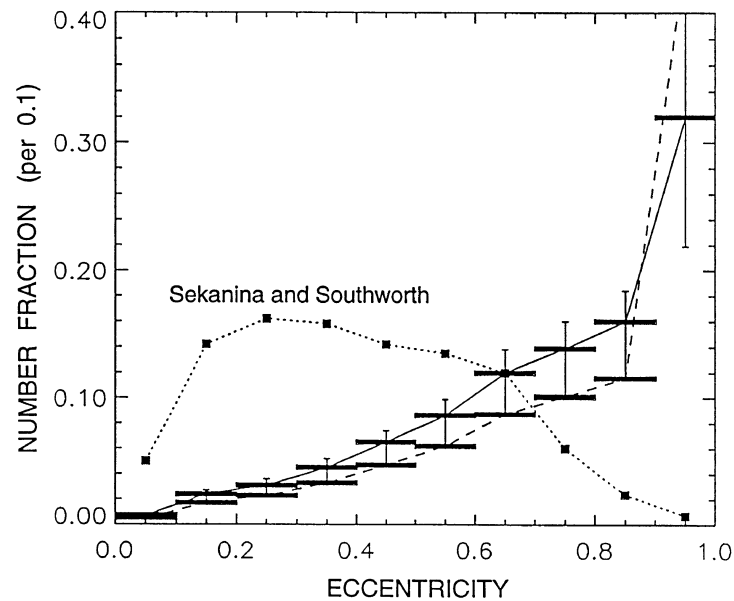


Fig. 5. The distribution of eccentricities of the orbits of meteoroids contributing to the radiant distribution in Fig. 4. Each orbit is weighted to account for the probability of a particle in the particular orbit colliding with the Earth. The dashed line is all the data; the full line shows the effect of removing about 20 orbits with extreme weights. The earlier distribution of Sekanina and Southworth (1975) bears no resemblance to the results of the present work.

Of the six sources identified in Fig. 4, the major ones are the helion and anti-helion contributed by meteoroids in prograde orbits, and the pair of apex sources contributed by meteoroids in retrograde orbits. The encounter speeds of ‘helion/anti-helion meteoroids’ range between 10 km/s and 40 km/s with a median value of 20 km/s, while the encounter speeds of the ‘apex meteoroids’ are 50–70 km/s with a median value of about 60 km/s.

The helion source shown on Fig. 4 is much weaker than the anti-helion source, although one would expect to encounter as many meteoroids in highly elliptical low inclination orbits moving away from the vicinity of the Sun (helion source) as there are moving toward the vicinity of the Sun (anti-helion source). In contrast to the HRMP results, Brown and Jones (1995) analysed meteor count rates surveyed during the early 1960’s, and concluded that the relative strengths of the helion and anti-helion sources were approximately equal. Further, within the uncertainties of their fits, the sporadic meteor sources are symmetric about the ecliptic and the apex-polar planes.

An explanation for the contradiction between the HRMP results and the work of Brown and Jones is to be found in the observations of Elford and Taylor (1997) who have shown that linearly-polarised meteor echoes observed during the day can be significantly attenuated due to the effect of Faraday rotation in the ionosphere. Under conditions of high solar activity and thus enhanced ionisation density in the day-time ionosphere, the Faraday effect could significantly reduce the radar echo count rate for the helion source in comparison to the echo rates associated with the anti-helion source. The data that Brown and Jones analysed were collected during a period of a minimum in the solar activity, while the HRMP data discussed here were collected in 1968–69 during sunspot maximum and are therefore highly susceptible to Faraday

day effect selection biases.

As we are uncertain of the value of the Faraday bias, we have not used the data described as the helion source but have assumed that the strength of this source is the same as that of the anti-helion source, and further that the radiant distribution is symmetrical about the plane orthogonal to the plane of the ecliptic and passing through the apex.

## 8. The Distribution of the Orbits in Space

The distribution in space of the orbits that contribute to the data presented in Fig. 4 is best described in terms of the distributions of the orbital elements. In presenting such distributions it is necessary to take into account the probability of a particle in a particular orbit undergoing a collision with the Earth. This is achieved by weighting the data according to a procedure described by Kessler (1981) who showed that for a meteoroid moving in an orbit that intersects the Earth’s orbit, the probability,  $P$ , of the meteoroid encountering the Earth is given by,

$$P \propto V(a^2 e \sin i \sin \varphi)^{-1}; \quad \cos \varphi = (a - 1)/(ae),$$

where  $a$ ,  $e$ , and  $i$  are the semi-major axis, eccentricity and inclination of the orbit, and  $V$  is the speed of encounter. The reciprocal of  $P$  is the ‘cosmic weight’ applied to each orbit of the data set.

The main features of the orbits: eccentricity, aphelion distance and inclination are given in terms of distributions in Figs. 5, 6 and 7.

• **Eccentricities** The distribution given in Fig. 5 indicates that the majority of the meteoroids orbits have eccentricities exceeding 0.4. As the Poynting-Robertson effect on the motion of particles is to decrease the eccentricity of their orbits there will be a tendency for points on this diagram to move from right to left over time, thus implying that the par-

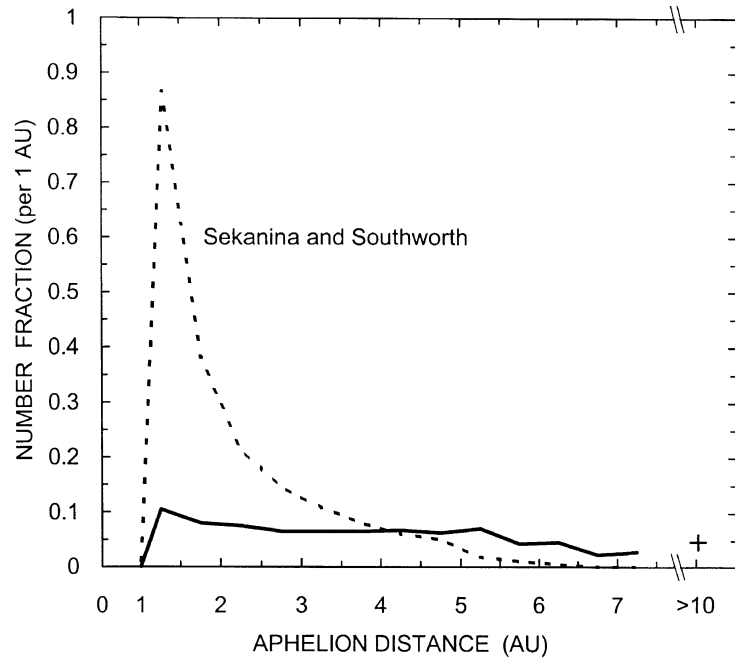


Fig. 6. The distribution of aphelion distances of the orbits of meteoroids contributing to the radiant distribution in Fig. 4. Each orbit is weighted to account for the probability of a particle in the particular orbit colliding with the Earth. The value at the right of the diagram is the sum of all the observations with aphelion distance  $>10$ . The effect of removing about 20 orbits with extreme weights made very little difference to the distribution of aphelion distances and is not shown. The earlier distribution of Sekanina and Southworth (1975) bears no resemblance to the results of the present work.

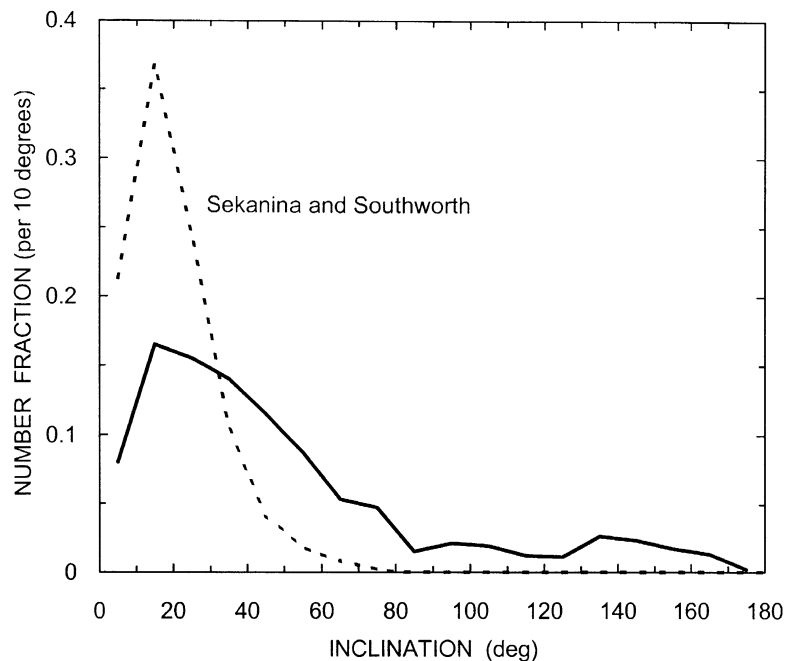


Fig. 7. The distribution of the inclinations of the orbits of meteoroids contributing to the radiant distribution in Fig. 4. Each orbit is weighted to account for the probability of a particle in the particular orbit colliding with the Earth. About 15% of the meteoroids move in retrograde orbits.

ent bodies of these particles must have even more eccentric orbits. The earlier distribution of Sekanina and Southworth (1975) bears no resemblance to the recent work.

• **Aphelion distances** From the distribution given in Fig. 6, it is clear that the mean aphelia of 3–4 AU is much larger than that estimated by the earlier workers. The small knee at 5.5 AU may indicate some degree of gravitational

influence by Jupiter on the original sources and on the subsequent orbital evolution of the meteoroid population. The value at the right of the diagram is the sum of all the observations with  $a > 10$ .

• **Inclinations** In the distribution given in Fig. 7, the effect of the cosmic weight is to enhance the proportion of orbits away from the ecliptic so that the mean inclination is

close to 40 degrees. There is also a significant fraction of orbits with inclinations exceeding 90 degrees; in fact the results imply that about 15% of meteoroids with masses  $>10^{-4}$  g (radius  $\sim 200$   $\mu\text{m}$ ) move in retrograde orbits. The distribution is very different from that derived by Sekanina and Southworth (1975).

## References

- Bronshten, V. A., *Physics of Meteoric Phenomena*, 356pp., Reidel, Dordrecht, 1983.
- Brown, P. and J. Jones, A determination of the strengths of the sporadic radio-meteor sources, *Earth, Moon and Planets*, **68**, 223–245, 1995.
- Elford, W. G., Calculation of the response function of the Harvard Radio Meteor Project Radar System, *Harvard Radio Meteor Project NASA Research Report*, no. 8, 1964.
- Elford, W. G. and G. S. Hawkins, Meteor echo rates and the flux of sporadic meteors, *Harvard Radio Meteor Project NASA Research Report*, no. 9, 1964.
- Elford, W. G. and A. D. Taylor, Measurement of Faraday rotation of radar meteor echoes for the modelling of electron densities in the lower ionosphere, *J. Atmos. Solar-Terr. Phys.*, **59**, 1021–1024, 1997.
- Grün, E., H. A. Zook, H. Fechtig, and R. H. Giese, Collisional balance of the meteoritic complex, *Icarus*, **62**, 244–272, 1985.
- Kessler, D. J., Derivation of the collision probability between orbiting objects: the lifetimes of Jupiter's outer moons, *Icarus*, **48**, 39–48, 1981.
- Lindblad, B. A., The IAU Meteor Data Centre in Lund, in *Interplanetary Matter; Proc. 10th European Reg., Meeting of the IAU, Prague*, edited by Z. Ceplecha and P. Pecina, **2**, 201–204, 1987.
- Lindblad, B. A., The IAU Meteor Data Centre in Lund, in *Origin and Evolution of Interplanetary Dust*, edited by A. C. Levasseur-Regourd and H. Hasegawa, Kluwer Acad. Publishers, 311–314, 1991.
- Love, S. G. and D. E. Brownlee, Heating and thermal transformation of micrometeoroids entering the Earth's atmosphere, *Icarus*, **89**, 26–43, 1991.
- Sekanina, Z. and R. B. Southworth, Physical and dynamical studies of meteors. Meteor-fragmentation and stream-distribution studies, *NASA Contractor Report CR-2615*, 94pp., Smithsonian Institution, Cambridge, Ma, USA, 1975.
- Southworth, R. B. and Z. Sekanina, Physical and dynamical studies of meteors, *NASA Contractor Report CR-2316*, 106pp., Smithsonian Institution, Cambridge, Ma, USA, 1973.
- Taylor, A. D., The Harvard Radio Meteor Project meteor velocity distribution reappraised, *Icarus*, **116**, 154–158, 1995.
- Taylor, A. D. and N. McBride, A radiant-resolved meteoroid model, *Proceedings, 2nd European Space Debris Conference*, 1997.
- Taylor, A. D., D. I. Steel, and W. G. Elford, Implications for meteoroid chemistry from the height distribution of radar meteors, *Adv. Space Res.*, **20**, 1501–1504, 1997.

---

A. D. Taylor (e-mail: andrew@meteors.demon.co.uk) and W. G. Elford (e-mail: gelford@physics.adelaide.edu.au)